NASA TECHNICAL TRANSLATION

NASA TT F-14,814

THE MARS-2 AND MARS-3 ORBITAL SPACECRAFT: RESULTS OF THE INVESTIGATION OF THE MARTIAN SURFACE AND ATMOSPHERE

V. I. Moroz

Translation of Orbital'nyye Apparaty Mars-2 i Mars-3: Rezultaty issledovaniy poverkhnosti i atmosfery Marsa, Author's manuscript, Moscow, 1973, 19 pp

NATIONAL AERONAUTICS AND SPACE ADMINISTRATION
WASHINGTON, D.C. 20546 FEBRUARY 1973

STANDARD TITLE PAGE

1. Report No. NASA TT F-14,314	2. Government Accession No.	3. Recipient's Catalog No.
4. Title and Subtitle THE MARS-2 AND MARS-3 ORBITAL SPACECRAFT: RESULTS OF THE INVESTIGATION OF THE MARTIAN SURFACE AND ATMOSPHERE		5. Report Date February 1973
		6. Performing Organization Code
7. Author(s) V. I. Moroz		8. Performing Organization Report No.
		10. Work Unit No.
9. Performing Organization Name and Address Leo Kanner Associates Redwood City, CA 94063		11. Contract or Grant No. NASW-2481
		13. Type of Report and Period Covered Translation
12. Sponsoring Agency Name and Address National Aeronautics and Space Administration, Washington, D.C. 20546		14. Sponsoring Agency Code

15. Supplementary Notes

Translation of Orbital'nyye Apparaty Mars-2 i Mars-3: Rezultaty issledovaniy poverkhnosti i atmosfery Marsa, Author's manuscript, Moscow, 1973, 19 pp

16. Abstract

Six differents were conducted on the Mars-2 and Mars-3 orbital spacecraft studying the Martian surface and lower atmosphere during and after a dust storm. Surface temperature, soil temperature, dielectric constant, relative altitudes at the planetary surface, surface brightness, H_2O content, and the density of the lower atmospheric neutral gas and the electronic density of the ionosphere were determined. Instruments used included an infrared radiometer, radiotelescope, CO_2 and H_2O photometers, and a photometer in the 3700-6940 Å range.

17. Key Words (Selected by Author(s))	18. Distribution Statement Unclassified - Unlimited		
19. Security Classif. (of this report) Unclassified	20. Security Classif. (of this page) Unclassified	21. No. of Pages 20	22. Price*

NASA-HQ

THE MARS-2 AND MARS-3 ORBITAL SPACECRAFT: RESULTS OF THE INVESTIGATION OF THE MARTIAN SURFACE AND ATMOSPHERE /1a*

V. I. Moroz

1. Introduction

Six different experiments to study the physical parameters of the surface and lower atmosphere of the planet were placed on board the Mars-2 and Mars-3 orbital spacecraft:

1) variation in surface temperature based on radiation in the 8-40 μm range [1,2,3],

2) variation in soil temperature at a depth of several tens of centimeters and variation in the dielectric constant based on radiofrequency radiation in the 3.4 cm wavelength [4],

3) determination of relative altitudes at the planetary surface based on the intensity of the CO_2 bands at about 2 μm [1,2,5],

4) photoelectric measurements of surface brightness in six narrow intervals from 3700 to 13,800 Å [1,2,6,7],

5) measurement of H_2O content in the atmosphere based on the intensity of the 1.38 μm absorption band [1,2,7], and

6) radio probing of the atmosphere to determine the density of the neutral gas in the lower atmosphere and the electronic density of the ionosphere [8].

The infrared radiometer and the photoelectric photometers for the CO_2 and H_2O bands and for selected regions of the continuous spectrum were described briefly earlier in the works [1,2,5,6,7,9]; Table 1 lists the main characteristics of all the instruments (field of view and measurement precision). The optical axes of all the instruments were parallel and the surface and atmospheric parameters were measured in the same planetary regions.

---

* Numbers in the margin indicate pagination in the foreign text.

Brightness in different ranges, surface and soil temperatures. /2
dielectric constant, altitude, pressure, and H_2O content in the atmosphere were obtained for the same regions.

The instruments were hard-mounted on the body of the AIS [automatic interplanetary station] and during the measurements they were oriented in a constant direction usually with the solar-stellar orientation system of the AIS. On approaching the pericenter of the orbit, the instruments were switched on for several minutes prior to transiting the limb, with a special optical sensor. The optical axes transited the planet usually along a line close to a great circle and the transit from limb to limb took about 30 minutes. Below we will refer to the trace of the optical axis on the planetary surface as the track of the measurements. From a preliminary estimate, the precision with which the measurement track was determined was 1-2° based on areographic coordinates.

In the experiments [1-5] all the results are from Mars-3. Its period of revolution was about 12 days. Fig. 1[1] shows seven measurement tracks made with this spacecraft.

The distance at the pericenter to the Martian surface varied somewhat as the orbit was evolved and was roughly in the range 1000-1500 km during this period. The first three transits, 15 December 1971, 27 December 1971, and 9 January 1972, took place during a dust storm and its abatement, and the remaining transits -- after the end of the dust storm. In December, January, and February the measurement tracks corresponding to successive dates of transiting the periares were shifted by about 90° in longitude with respect to each other. As a result, sizable sections of the 3 February 1972, 16 February 1972, and 28 February 1972 tracks past close to the 15 December 1971, 27 December 1971, and 9 January 1972 tracks, and we have measurements for the same Martian regions obtained during the storm (more exactly, during its last stage) and after the storm. The 12 March 1972 track could not,

TABLE 1 MAIN CHARACTERISTICS OF INSTRUMENTS

Instrument	Function	Field of view[1], km	Wavelength, μm	Band Width, μm	Range of measurements	Internal accuracy	Accuracy of absolute calibration
Infrared radiometer	Measurement of brightness temperature of surface, T_e	30	8-40	~30	150-300° K	± 2° at 250° K ± 10° at 160° K	± 5° at 250° K ± 10° at 160° K
Radiotelescope	Measurement of soil temperature, T_{ss}, and dielectric constant, ε	100	3.4 cm		< 300° K	± 20 % for T_{ss} 10-50% for ε	
CO_2-photometer	Measurement of ratios of pressures P and altitude difference Z based on CO_2 band intensity	15	2.014 2.050 2.057 2.075 2.25	0.02 0.02 0.02 0.02 0.02	1-50 mbar ± 20 km	±0.3-1.0 mbar for P ±0.5-±2 km for Z	
H_2O-photometer	Measurement of H_2O content in the atmosphere (U_D) and brightness in the continuous spectrum near the H_2O band (1.38 μm)	7.5	1.38	0.006	0.5-100 μm of precipitated water $2\text{-}1200 \cdot 10^{-5}$ $w \cdot cm^{-2} \mu m^{-1} ster^{-1}$	±0.5 ±2 μm $\pm 2 \cdot 10^{-5}$ $w \cdot cm^{-2} \mu m^{-1} ster^{-1}$	Factor of 2 [2] ±20%
Photometer in the 3700-6940 Å range	Measurement of brightness (B_λ) of selected narrow regions of the continuous spectrum	45	0.370 0.416 0.494 0.552 0.694	0.03 0.006 0.005 0.007 0.011	$0.1\text{-}2000 \cdot 10^{-5}$ $w \cdot cm^{-2} \mu m^{-1} ster^{-1}$	±10% [3]	±20%

FOOTNOTES: [1] Corresponds to the radiation pattern at the 0.5 level, a distance of 1500 km, and a zero zenith angle of the orbital spacecraft. For the CO_2-photometer and the visual-range photometer, measurements were taken at an interval of 36 sec (140 km, at the pericenter) and were averaged at an interval of 12 sec (about 50 km). Continuous profiles were recorded in the remaining cases.

[2] It is proposed that the absolute calibration for H_2O be refined by additional laboratory measurements.

[3] Large errors due to scale nonlinearity (logarithmic photometer) were not excluded.

/16

for a number of reasons, be tied into the surface with sufficient reliability and its position as shown in Fig. 1 must be considered as approximate.

Overall, the volume of information obtained with Mars-3 was somewhat less than with Mariner-9. However, experiments were /3 conducted on Mars-3 which were generally not included on Mariner-9 (photoelectric photometry in the near infrared and visible spectral regions and radioastronomical measurements), while as for the experiments similar to those conducted on Mariner-9 (IR-radiometry, optical altimetry, and H_2O content measurement), the Mars-3 results are of interest not only as supplementary material since -- firstly -- they afford an integrated consideration together with photometric and radioastronomical data, and -- secondly -- they were taken with widely different methods.

In particular, the measurement of the H_2O content and CO_2-altimetry in our experiments were made for bands lying in the near infrared region, and the measurement results are practically independent of the vertical temperature distribution. Bands in the far infrared spectral region were used on Mariner to get the same data, and these bands depend so strongly on the vertical temperature profile that they can be observed both in emission as well as in absorption /10/. Though the analysis of the spectra obtained with the IRIS /infrared interferometer-spectrometer/ simultaneously yields also the vertical temperature profile, the problem is greatly complicated and, probably, does not always admit of a unique solution. The topographic material obtained with Mariner-9 using ultraviolet photometry /11/ is very valuable due to the globality of the coverage, but requires a cauticus approach since it is strongly subject to the effect of inhomogeneities in the atmospheric dust content.

Below we propose to briefly review already published data and present new results. They apply to the first six Mars-3 sessions.

We are indebted to N. N. Krupenic and I. B. Drozdovskaya for giving us the results of the radioastronomical experiments before publication.

We are also indebted to D. Shneiderman (NASA) for the Mariner photographs of the Martian surface in the regions extending along the Mars-3 measurement tracks. In several cases they /4 assisted in the interpretation of measurements. Their comparison with photometric curves confirmed that the tracks were determined with the above-indicated accuracy of 1-2°, and in the following the track position can be calculated with the aid of the Mariner photographs.

2. Direct Results of Measurements

Figs. 2-7 give the results of measurements along six tracks pertaining mainly to the surface. The brightness infrared temperature T_B, soil temperature T_{ss} (at a depth of several decimeters) measured on the basis of radiofrequency radiation at a wavelength of 3.4 cm, dielectric constant ϵ, brightness in the continuous spectrum (photometric profile) in the near infrared region B (1.4 μm), and altitude Z relative to the 6 mbar level are presented. Here are also given, for comparison with the results of the measurements, the values of μ_1 -- the cosine of the solar zenith distance -- and $\overline{T_s}$ -- the theoretical mean-diurnal surface temperature.

Fig. 8 presents separately the altitudes for 27 December 1971. They are separated because over much of the track they clear refer not to the surface, but to the cloud cover

Figs. 9-14 concentrate the results pertaining mainly to the atmosphere: pressure P, H_2O content profile, and brightness (photometric profile) in the near ultraviolet region of 3700 Å. Here also are given the brightness at the wavelength of 4940 Å, determined by scattering both by the surface and the atmosphere, and the brightness at the wavelength of 6940 Å, determined by scattering mainly by the surface (just as for 1.4 μm). The

latter remark is valid only for measurements taken after the end of the dust storm. During the 15 December 1971 and the 27 December 1971 tracks the brightness in both the red and near infrared regions was due significantly to reflection from dust clouds.

The method of processing infrared temperatures is given in the papers [1-3]. We recall that a wide-band filter was used in /5 our radiometer and in the region of the fundamental CO_2 absorption band (λ =15 μm) the radiation was determined by the atmosphere, which can be colder or warmer than the surface -- depending on specific conditions. To take into account the atmospheric effect in the first approximation, in the neighborhood of the 15 μm band we increased the measured fluxes by 5 percent (which gives a correction of about 1 percent in the temperature). Actually, the magnitude and sign of this correction depend on the local time, atmosphere model, and the zenith angle of the craft. Below we will suggest determining the correction for absorption more exactly.

The brightness infrared temperature T_B is very close to the kinetic temperature of the surface layer T_s. And actually, by neglecting the difference between T_B and the effective temperature T_e, we have

$$T_B^4 = B_1 T_s^4 \qquad (1)$$

where B_1 is the coefficient of radiation in the infrared range. Laboratory measurements [12] for earth minerals yield $B_1 \simeq 0.95$, so that if we assume the same value for Mars, the difference between T_B and T_e and T_s will be of the order of 1 percent. The ratio T_B/T_s depends weakly on B_1, as the root of the fourth power. The situation is even weaker in the radiofrequency range, where the following relationship holds:

$$T_B = B_2 T_{ss} \qquad (2)$$

Here the error due to indeterminacy in the knowledge of B_2 (the coefficient of radiation in the radiofrequency range) is somewhat

greater. However, the radiofrequency experiment was constructed in such a way (measurement in two polarizations) that it permitted determining B_2 and T_B separately. In processing the observations, it was assumed that the Martian surface can be represented as a smooth sphere. The coefficient of radiation for the sum of the two polarizations in this case is equal -- by Fresnel's law -- to

$$B_2 = 1 - \frac{\tan^2(Z' - Z)}{\tan^2(Z' + Z)} - \frac{\sin^2(Z' - Z)}{\sin^2(Z' + Z)} \qquad (3)$$

where Z is the zenith angle of the craft, and Z' is determined /6
from the relationship

$$\frac{\sin Z}{\sin Z'} = n = \sqrt{\epsilon} \qquad (4)$$

Figs. 2-7 give the values of T_{ss} and ϵ separately. The errors in the determination are evidently due to the disparity of the actual surface from the adopted hypothesis of a smooth sphere. The too large and too small values lead to overstating and understating T_{ss}, respectively. We can discard these out-of-line points if we compared T_{ss} with the mean-diurnal temperature of the surface $\overline{T_s}$. It must be anticipated that these values will be close to each other for Martian soil. In Figs. 2-7 we plotted the $\overline{T_s}$ values calculated by the formula

$$\overline{T_s} = \left(\frac{E_0}{\sigma r^2} \frac{1 - A}{B_1} \overline{\cos Z}\right)^{1/4} \qquad (5)$$

where $\overline{\cos Z}$ is the mean-diurnal cosine of the zenith angle of the sun, A is the integral albedo, E_0 is the solar constant, and r is the distance to the sun in astronomical units. We assumed $\frac{1 - A}{B_1} = 1$. On the average, the T_{ss} values lie roughly 20° below the $\overline{T_s}$ curve, which can be attributed to calibration inaccuracy.

The method of determining pressures and relative altitudes is given in the works [1,2,5] and the method of water content determination is found in [7].

Brightness B measurements were taken only in relative terms, but here it is essential that the brightness scale is the same for all sessions. Absolute brightness units plotted on the ordinate axes for 1.38 μm were obtained on the assumption that for 16 February 1972 and 28 February 1972 sessions the brightness in the light regions is subject to Lambert's law, and the brightness coefficient (visible albedo) for the light regions is 0.41.

The fact that on Mars during the period when the measurements were begun, the dust storm still continued has both negative and positive aspects. A negative aspect is obvious: the presence of dust clouds interferred with the photographing of the surface and reduced the possibilities of several optical experiments (H_2O and CO_2-photometers) during several of the first sessions. Even so, the dust storm brought a benefit, since never before were there as great opportunities for studying the nature of this tremendous and puzzling phenomenon. [7]

3. When Did the Storm Begin and How Much Did It Affect the Results of Measurements

Relevant phototelevision images on Mariner were obtained systematically since late in December, however as far as we can judge from the photographs we have at hand the transparency of the Martian atmosphere continued to increase during this period.

How transparency varied with time can be traced from our photometric profiles. Table 2 gives the mare-highland contrasts for 1.38 μm in different sessions. Here are also given the cosines of the zenith angles of the sun and the craft (μ_1 and μ_2) and the phase angles α. The contrasts represent the ratio $\frac{B_c - B_m}{B_c}$, where B_m is the mare brightness (solid curve), and B_c is the brightness of the highlands (dashed curve), yielding the

Lambertian interpolation of the brightness level corresponding to the highlands. Table 2 also gives the values of the highlands brightness R_{max} corresponding to the dashed [illegible]e for each track. Obviously, in general they are systematic[illegible]y r[illegible]ed; on 15 December R_{max} was 15 percent greater than in the two last sessions in February.

TABLE 2

Session	$\frac{B_c - B_m}{B_c}$		ϕ	λ	μ_1	μ_2	α	R_{max}
15 Dec 71	0.25	M. Cimmerium	-30	222	0.457	0.976	52	0.47
27 Dec 71	0.32	Iapigia	-26	304	0.535	0.992	53	0.45
9 Jan 72	0.51	M. Erythraeum	-23	29	0.606	0.999	54	0.44
3 Feb 72	0.39	M. Cimmerium	-30	215	0.826	0.855	56	0.45
16 Feb 72	0.56	Iapigia	-25	299	0.872	0.816	57	0.41
28 Feb 72	0.55	M. Erythraeum	-25	30	0.671	0.915	59	0.41

On 9 January 1972 the mare-highland contrast values were now close to the values reached in the February sessions, though the difference was still present.

Atmospheric transparency clearly depends on latitude. At latitudes south of 50° in the 15 December and 27 December sessions the profile B (1.38 μm) contains a large number of fine details, while closer to the equator there are no details and the maria have the appearance of smooth minima. On 15 December, the red profile (6940 Å) showed Prometei Sinus, but Mare Cimmerium was altogether absent from it.

The general impression is that on 15 December and 27 December 1971 the dust content of the atmosphere was so high that the results of measuring pressure, altitude, and H_2O content for latitudes north of −40° were greatly impaired by the dust storm. There is some uncertainty also in similar results for 9 January 1972. So the curves of pressures, altitudes, and H_2O content for the first sessions are plotted with dashed lines, and for

27 December 1972 these curves are not given at all, since in this session the equivalent CO_2 bandwidths were especially small. In another figure (Fig. 8) are given the altitudes for this session; in the following they will be used in determining the altitude of the upper cloud ceiling.

The altitudes determined in the 15 December 1971 and 9 January 1972 sessions can probably be used with caution in the role of some qualitative characteristic of the relief.

The infrared temperature found from radiation in the 8-40 μm range pertains to the surface even for the December sessions. Two arguments can be cited favoring this conclusion:

1) Atmospheric transparency clearly increases with wavelength in the transition from 0.7 to 1.4 μm. If this is attributed to small particle sizes, which is most highly probable, then for the radiation at $\lambda > 8$ μm the dust clouds must be completely transparent. /9

2) The dependence of temperature on local time correlates quite well with the theoretical dependence calculated without allowance for the atmospheric radiation. There is only the difference that the measured temperature curve lies somewhat below the theoretical curve, accounted for by the absorption of solar radiation in the clouds [1,2,3,6]. This means that the optical thickness of the dust clouds is small in the vicinity of $\lambda > 8$ μm.

4. Martian Surface: Temperature, Soil Density, and Altitudes

Temperature and thermal properties of the surface layer

The theoretical effective surface temperatures T_e were calculated for different values of the thermal inertia $(k\rho c)^{1/2}$ for values of the integral albedo $A = 0.25$ (light regions) and $A = 0.15$ (dark regions). The T_B profiles for 16 February and 19 February 1972 are satisfactorily approximated by theoretical curves with $(k\rho c)^{1/2} = 0.006$ cal·cm^{-2}·sec$^{-1/2}$·deg^{-1} (Figs. 15 and 16). An exception is represented by the latitudes $\phi > +40^\circ$ where the measured temperatures are very much below

the theoretical temperatures and are close to the condensation temperature of CO_2 at the latitudes $\phi \geq \mp 50^\circ$.

An increased therm[illegible]ertia constant (0.008) was found in the area of the compact dark region Cerebrus. Obviously, there is a well-defined correlation between T_B and brightness B (1.38 μm). Regions with lower brightness (lower reflectivity) have higher temperatures.

In the dust storm period (15 December and 27 December 1971) the surface temperature was below "normal" [1,2,3,6]; this is also indicated by the Mariner measurements [13] and terrestrial observations by the author and his coworkers [14].

Temperature, dielectric constant, and soil density (results of radioastronomical experiment)

The soil temperature at a depth of several decimeters correlates satisfactorily with the calculated mean-diurnal temperatures. As to be expected, there are no signs of diurnal soil /10 temperature fluctuations. If sections where the temperature T_{3s} differs widely from the calculated temperature T_3 are discarded, the mean value of the dielectric constant is

$$\epsilon \approx 4 \pm 1,$$

which corresponds to the normal (Z = 0) coefficient of radiation $\epsilon = 0.9$.

The dielectric constant for most anhydrous earth minerals, as shown by Krotikov [15], is related to the soil density ρ by the relationship

$$\rho = 2 (\sqrt{\epsilon} - 1) \cdot g \cdot cm^{-2} \qquad (6)$$

whence we have the following estimate for the density of Martian soil

$$\rho = 2 \ g \cdot cm^{-2}.$$

By comparing B (1.38 μm) and ϵ for the tracks from 9 January 1972 to 28 February 1972, we can see that in the dark regions there is a tendency toward an increase in ϵ (and thus, density).

Altitudes

Altitude profiles also correlate with brightness -- to a lesser extent than do infrared temperatures, but the correlation unconditionally does exist. This correlation is not always well-defined and no attention was given to it in the first publications [1,2,5]. By comparing altitude profiles and brightness profiles, in Figs. 2-7 we can still see that the darker regions are generally higher than the neighboring lighter regions.

Altitudes relative to the 6 mbar level in our tracks were in the limits -1.5 to 6 km. The highest regions are located in Mare Australe (9 January 1972 track), Syrtis Major (16 February 1972 track, about 4 km), Nereidum Fretum (28 February 1972 track, about 4 km), and the lowest are in Umbra (16 February 1972 track, about -1 km) and Chrise (28 February 1972 track). The tracks of 16 February and 28 February 1972, extending far into the northern latitudes, show a tendency toward a systematic lowering of altitudes in the northern hemisphere. This is also shown by the radio occultation observations of Mariner [15].

5. Martian Atmosphere: Pressure, Water Vapor, Dust Storm, and High-Latitude Clouds /11

Pressure

Absolute pressure values determined from our observations are not reliable enough for final conclusions; however, the impression is obtained that the value of 6 mbar is somewhat higher than the mean value. The mean value is evidently closer to 5-5.5 mbar. Pressures measured for all tracks fluctuates within the limits 3.5 to 7 mbar.

Radio occultation observations of Mars-2 yield pressures of 5-10 mbar [3]; these results will obviously be refined.

Water vapor

Along the tracks of 16 February 1972 and 28 February 1972 the water vapor content in the atmosphere reached u_0 = 6-8 μm of

precipitated water. Mariner-9 [12] and terrestrial observations conducted simultaneously [16] yield about 10 μm of precipitated water on the average for Mars. The agreement can be regarded as satisfactory, considering the possibility of geographic and time variations (and also changes in our calibrations). The rise in u_0 in the period from December to February, found by measurements on Mars-3, was independently confirmed by terrestrial observations [16]. There is some correlation between water content in a vertical column and pressure, as must be the case in the absence of saturation (the relative humidity was of the order of several percent) everywhere, with the exception of the cold regions in the northern hemisphere. The abrupt drop in humidity at latitudes north of $+50^{\circ}$ was accompanied by the formation of near-polar clouds strongly scattering UV-radiation (cf. Fig. 13). On the average, the water vapor content in the Martian atmosphere in the measurement period was several times less than in the same season as shown by terrestrial observations during the period of the preceding oppositions.

Dust storm

Here we will deal with three problems -- altitude of the clouds, particle sizes, and the effect of the dust storm on the thermal conditions of the surface. /12

a) Cloud altitude

Very low pressure (down to 2 mbar) and altitude (down to 10-15 km) values were obtained for the 27 December 1971 track (in the zone lying north of -30°) after processing of the CO_2-photometer observations using the standard method. It is natural to assume that these pressures and altitudes refer to some effective reflecting level in the clouds. Thus, their altitude proves to be of the order of the altitude of the homogeneous planetary atmosphere. Similar results were obtained in the terrestrial observations of the author and O. G. Taranova [17], and also by Parkinson and Hunten [18]. The distribution of temperature with

Our estimate is based on the simple fact that the transparency of the clouds at the 1.4 μm wavelength is markedly higher than at the 0.7 μm wavelength. This is especially clearly evident from a comparison of the red (0.694 μm) and infrared (1.38 μm) profiles of 15 December 1971. Since the cloud albedos (and thus also the true absorption) at these wavelengths are nearly identical, the difference in transparency can be attributed only to the quite small ratio of radius to wavelength. An approximate quantitative consideration yields the estimate indicated above, $r \simeq 1$ μm.

The optical thickness

$$\tau = \int_0^\infty \alpha_Z \, dZ$$

(where α_Z is the coefficient of extinction) must be about 3 for 1.4 μm and more than 6 for 0.7 μm in order to explain the 15 December 1971 observations at this radius.

It is very important not to err in the mean estimates of particle size for the entire concept of the dust storm. If particle sizes are of the order of 1 μm, the particles can be suspended in the atmosphere for about 100 days and strong vertical movements in the atmosphere are not required for protracted persistence of the dust clouds. In this case, the dust storm is a storm in the common sense of the word only in the initial stage, /14 but then the wind velocity is reduced and the second phase -- the phase of slow settling -- sets in.

But if the estimate of Leovy et al. is valid and the particles are larger, the settling time is only several days and there must be strong atmospheric movements throughout the period in which the dust clouds are observed for the dust clouds to persist.

The optical thickness $\tau \simeq 3$, $r \simeq 10^{-4}$ cm with the density $\rho \simeq 3$ g/cm^2 yield a mass of dust in a column 1 cm^2 in cross-section of about 10^{-3} g/cm^2, which corresponds to a mass of dust weighing 10^9 tons in the atmosphere of the entire planet.

c) Effect of the dust storm on the planetary thermal regime

As indicated, the surface temperature during the dust storm decreases. This is a consequence of the higher transparency of the dust clouds for the departing longwave planetary radiation than for the shortwave solar radiation. It is natural to call this effect the antigreenhouse effect, since it is opposite in sign to the greenhouse effect. A semiquantitative analysis of the planetary thermal balance when the antigreenhouse effect is present has been presented in a work by Ginzburg /21/.

High-Latitude Clouds

On the 16 February 1972 and 28 February 1972 tracks the ultraviolet profiles showed a sharp rise in brightness upon transiting the latitude at about 35-40°. Mariner photographs obtained in the same regions, several days later, demonstrate bright clouds here. These clouds show up practically not at all in the near infrared spectral region, from which the following may be concluded:

1) particle sizes are small (tenths of a micron), and

2) the clouds are entirely transparent to surface radiation in the far infrared region, and the temperature measured here pertains to the surface.

Though the surface temperatures in this region are close to the CO_2 condensation point, it is not necessary that the high-latitude clouds consist of solid carbon dioxide, since here a temperature inversion in the atmosphere is possible. From the H_2O profiles we can see that water vapor disappears here. Five to ten microns of precipitated water in the form of small-radius ice particles can provide optical thicknesses $\tau \geq 1$, occurring in the shortwave region of the spectrum. /15

altitude obtained in two Mariner experiments (IRIS, cf. [10]) and radio occultation measurements [15] independently indicate a high cloud altitude.

b) Estimate of particle sizes

We will dwell on this problem in greater detail, since here there are contradictions between different authors. Moroz et al [1,2,7] give the estimate

$$r \simeq 1 \quad \mu m \quad .$$

Pang and Hold indicate a close value [19]:

$$r \simeq 2 \quad \mu m \quad .$$

Leovy et al. give a much larger radius [20]:

$$r \simeq 10 \quad \mu m \quad .$$

All three estimates are based on photometric arguments. Of course, dust clouds are inhomogeneous in different regions and at different altitudes particles of different sizes can be present. However, the method used by the author's [20] raises fundamental objections. Their considerations amount to the following:

1) The albedo of clouds in the visual spectral region is small ($\simeq$ 0.13), which means that the albedo of single scattering is small, and the single-scattering albedo is the smaller, the larger the particle size. Without presenting their calculations, the authors [20] state that the albedo observed can be attained only for dimensions of several tens of microns. /13

2) There are photometric and radiometric arguments in favor of the view that the surface layer consists of grains several tens of microns in size. The authors [20] believe it is natural to expect that dust clouds consist of particles of the same size.

Both arguments do not appear convincing to us. The same particles have much larger albedo values of single scattering in the red and near infrared spectral regions, and the sizes of surface layer grains obviously can be much larger than the mean size of particles suspended in the atmosphere.

REFERENCES

/16

1. Moroz, V. I. and Ksanfomaliti, L. V., Vestnik AN SSSR, No. 9 (1972).

2. Moroz, V. I. and Ksanfomaliti, L. V., Icarus 17:408 (1972).

3. Moroz, V. I., Ksanfomaliti, L. V., Kasatkin, A. M. et al., Doklady AN SSSR 208, No. 2 (1973).

4. Basharinov, A. E., Drozdowskaya, I. B., Egorov, S. T. et al., Icarus 17:540 (1972).

5. Moroz, V. I., Ksanfomaliti, L. V., Kunashev, B. S. et al., Doklady AN SSSR 208, No. 5 (1973).

6. Moroz, V. I., Ksanfomaliti, L. V., Kasatkin, A. M., and Nadzhip, A. E., Kosmicheskiye issledovaniya 9, No. 6 (1972).

7. Moroz, V. I., Nadzhip, A. E., and Gil'varg, A. B., Doklady AN SSSR 208, No. 4 (1973).

8. Koloso., M. A., Yakovlev, O. I., Kruglov, Yu. M. et al., Doklady AN SSSR 206:1071 (1972).

9. Ksanfomaliti, L. V., Pribory i tekhnika eksperimenta, No. 4, 192 (1972).

10. Hanel, R., Conreth, B., Hovis, W. et al., Icarus 17: 423 (1972).

11. Hord, C. W., Barth, C. A., Stewart, A. I., and Lane, A. L., Icarus 17: 443 (1972).

12. Hovis, W. A. and Callahan, W. R., JOSA 56: 639 (1956).

13. Chase, S. C., Hatzenbeler, J., Kieffer, H. H. et al., Science 175:305 (1972).

14. Liberman, A. A., Moroz, V. I., and Khromov, G. S., Astron. tsirk., No. 705, 5 June 1972.

15. Cliore, A., Caine, D. L., Fjeldbo, G. et al., Icarus 17: 484 (1972).

16. Tull, R. G. and Barker, E. S., Bull. Am. Astron. Soc. 4, No. 3, 11 (1972).

17. Moroz, V. I. and Taranova, O. G., Astron. tsirk., No. 697, 10 May 1972. /17

18. Parkinson, T. D. and Hunten, D. M., Science 175: 323 (1972).

19. Pang, K. and Hold, C. W., Mariner-9 Ultraviolet Experiment: 1971 Mars Dust Storm, University of Colorado, 1972.

20. Leovy, C. B., Briggs, G. A., Young, A. T. et al., Icarus 17:373 (1972).

21. Ginzburg, A. S., Doklady AN SSSR, 208, No. 3 (1973).

CAPTIONS TO FIGURES

Fig. 1. Measurement tracks of Mars-3. /18

Fig. 2. Results of measurements along the 15 December 1971 track. Brightness infrared temperature T_B, soil temperature (calculated from radiofrequency radiation), T_{SS}, brightness B (1.4 μm) in the continuous spectrum near 1.4 μm, dielectric constant of soil ϵ, altitude Z relative to the 6 mbar level, $\overline{T_s}$ -- calculated mean-diurnal temperature, and μ_1 -- cosine of zenith distance of the sun.

Figs. 3-7. As above, for the remaining five tracks from 27 December 1971 to 28 February 1972.

Fig. 8. Altitudes based on 27 December measurements. In the right part, the altitudes undoubtedly refer to the upper cloud ceiling, and not to the surface. Altitudes along the coincident section of the 16 February 1972 track are given by the dashed line.

Fig. 9. Results of measurements along the 15 December 1971 track. The H_2O content, pressure, brightness at the wavelengths of 6940, 4940, and 3700 Å, μ_1 -- cosine of the zenith distance of the sun, and μ_2 is the cosine of the zenith distance of the spacecraft.

Figs. 10-14. As above for the remaining five tracks.

Fig. 15. Comparison of measured and calculated temperatures for the 16 February 1972 track.

Fig. 16. As above for the 28 February 1972 track.

FOOTNOTES

[1] Figs. 1-7 and 9-16 are missing.

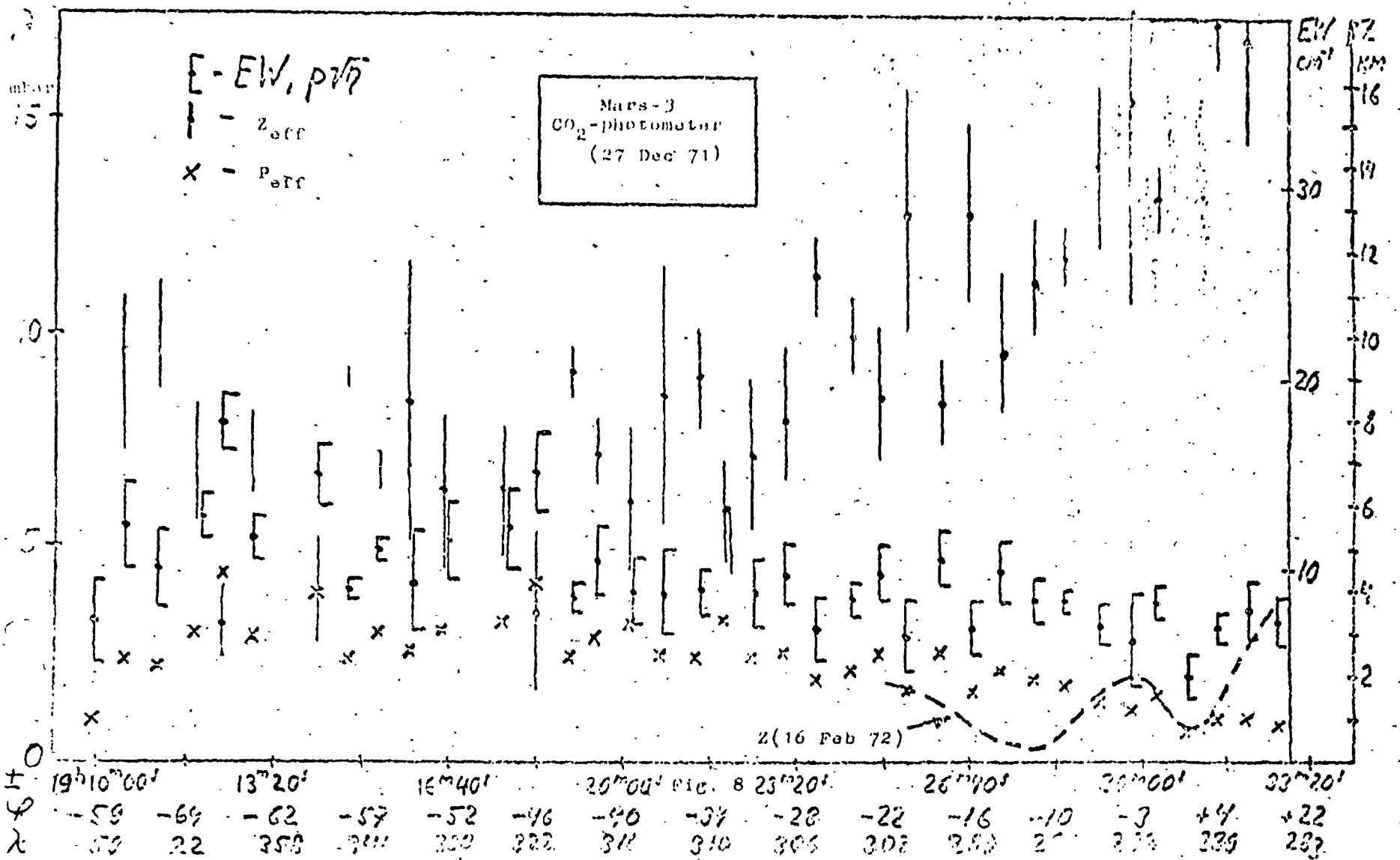
[- EW, p√η
| - z_eff
× - P_eff
Mars-3
CO2-photometer
(27 Dec 71)
z(16 Feb 72)
EW cm⁻¹
z km
mbar
19h10m00s
13m20s
16m40s
20m00s
23m20s
26m40s
30m00s
33m20s
φ -59 -64 -62 -57 -52 -46 -40 -34 -28 -22 -16 -10 -3 +4 +22
λ 22 355 339 332 310 309 283 239 237

Fig. 8

/19